

# BEHAVIOUR OF A PISTON CORER FROM ACCELEROMETERS AND NEW INSIGHTS ON QUALITY OF THE RECOVERY

Jean-François Bourillet, Gilbert Damy, Loïc Dussud, Nabil Sultan and Patrice Woerther  
*Ifremer, France*

Sébastien Migeon  
*Geosciences Azur, France*

## Abstract

Various observations pointed out that cores performed with gravity piston corer show significant distortions mainly located at the top of the core. A series of 15 cores were performed at the same location on a submarine sand wave (Var canyon, France). Six different settings of the corer – three freefall heights and three slacks of the piston cable – were tested, including duplicates. Two accelerometers recorded simultaneously the movements of the core tube and the movements of the triggering arm. Then the  $z$  displacements were obtained by a double integration versus time of the measured acceleration. The analyses of results allowed the authors to estimate the amplitude and the duration of the elastic recoil of the aramid cable, and to distinguish four steps during the 4 seconds of penetration, including a distortion phase followed by a normal sampling phase linked to the status of the piston.

The analyses of the quality and benchmark layers from recovered cores highlight the major role of the piston driven by the lengths of the counterweight and piston cables. The recovered thickness of a given layer can vary from 0.8 to 1.3 depending to the settings.

A cone penetrometer test (CPT) trial at the same location gives a good estimation of the absolute geometry of the layers. The settings for cores with geotechnical purpose (better quality) will be different from settings for cores with sedimentological or palaeoclimatological purposes (better geometry). A compromise is proposed.

## 1. Introduction

Gravity coring with stationary piston is an efficient way to recover long sedimentary cores<sup>1</sup>. However, various observations pointed out consequent distortions<sup>2</sup> based on different techniques: magnetic orientation<sup>3</sup>, and comparison of different corers or with sub-bottom profiler<sup>4</sup>. Authors described the ‘over-sampling’ and the ‘under-sampling’<sup>5</sup>, and others proposed recommendations for improvements of corers<sup>6</sup>.

The Stacor corer gets round these disturbances with a truly stationary piston<sup>7, 8</sup>. The device provides high quality sampling<sup>9</sup> especially for soil investigation<sup>10</sup>. But the duration of the deployment (8–10hr) and the size of vessels and cranes are constraining factors for the use of such a device by scientific community.

The trial of a new aramid cable onboard the R/V *Le Suroît* was an opportunity to examine the effect of the elastic recoil of such a cable on the recovered sediment. The use of accelerometers allowed for the recording the behaviour of a corer and understanding the effect of settings on the recovered sediment.

## 2. Method

### 2.1 Devices and sensors

The stationary piston corer of the R/V *Le Suroît* consists of a 994kg weight and a 10m steel tube with a plastic liner

(maximum recoverable length of sediment of 9.55m), as well as a platform for the release or triggering arm linked to the main cable and the counterweight linked to the platform with a cable (Figure 1). The piston is linked to the platform via the piston cable and slides freely inside the liner. The main cable is a 17mm aramid cable with a weight in water of 0.056kg/m.

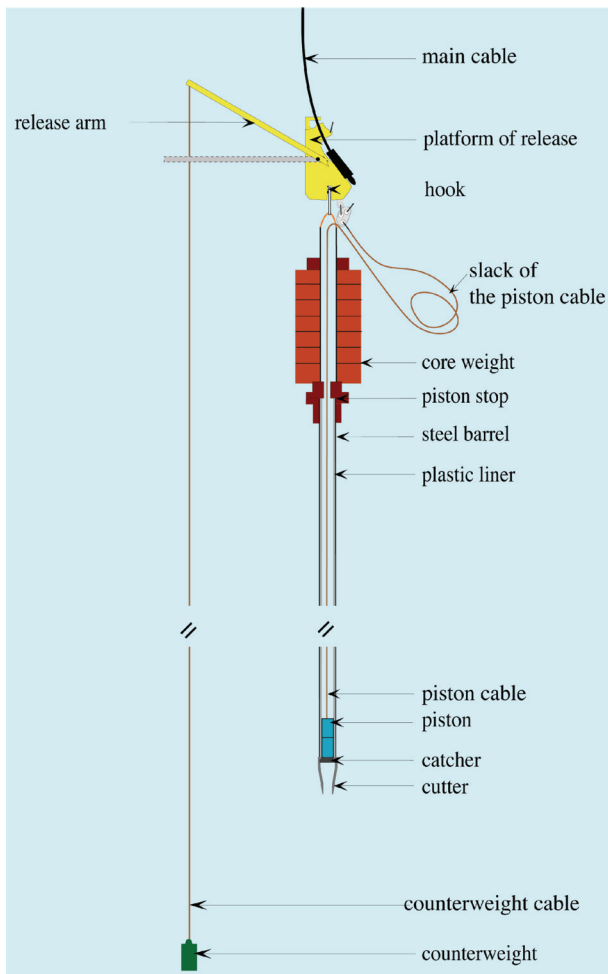
Two autonomous accelerometers from Micrel Company equipped the top of the weight and the flank of the platform. These devices record the acceleration along the  $x$  and  $z$  axes,  $\pm 2g$  at 50Hz, and the  $x$ ,  $y$  and  $z$  axes,  $\pm 20g$  at 50Hz, respectively.

The Penfeld penetrometer allows measuring geotechnical parameters at maximum depth of 6000m. This standard 36mm CPT device was deployed during its sea acceptance test onboard the R/V *Atalante*<sup>11</sup>.

### 2.2 Methodology

The influence of different parameters is tested by individually changing each of the different parameters at the same location on a submarine sand wave (Var canyon, France). Three heights of freefall and three recoil compensation representing six different trials are tested and each trial is duplicated once or twice (Table 1). The slack of the piston cable

Figure 1: Sketch of a piston corer



is the sum of the freefall height and the length selected to compensate for the elastic recoil of the main aramid cable.

Thus 15 cores are recovered during the ESCAR7 cruise. For each core, a sedimentological log is established, and the depths of the reference levels are measured. The processing of the accelerometers records provide the following curves: acceleration along the x, y and z axes; velocity of the core weight along the z axis; displacement of the core weight along the z axis; velocity of the platform along the vertical axis; and displacement of the platform along the vertical axis. The velocity curve is based on an integration of the acceleration versus time; the displacement curve is based on a double integration of the acceleration versus time.

The Penfeld CPT tool dives at exactly the same location during the PENETRESS cruise. The combination of density, tip resistance, friction and excess pore pressure allows classifying the soils. The estimated lithology log is used as reference for the geometry of the cored layers.

### 3. Results

#### 3.1 CPT trial

It is possible to classify soils due to CPT measurements<sup>12, 13</sup>. The interpretation of the Penfeld dive allows for the determination of 9 levels. The depths and thicknesses are used as references (Figure 2).

#### 3.2 Corings

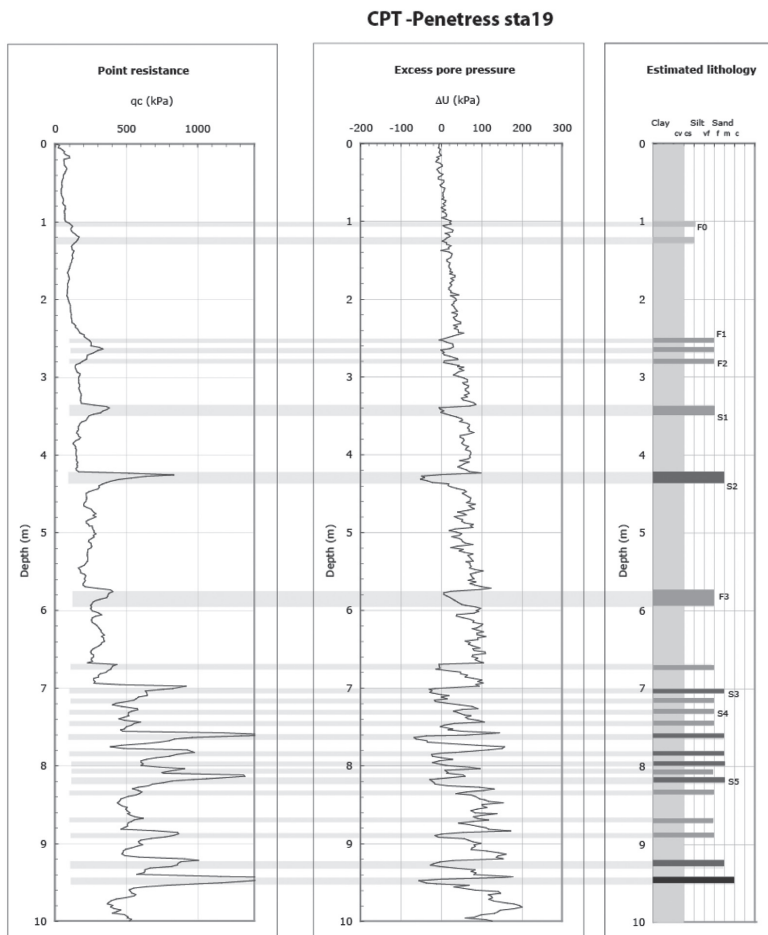
The observed penetration indicates that all successful corings except one penetrated the sediment between 9 and 10m (Table 1). The comparison between observed and computed penetrations from the accelerometers shows an underesti-

Table 1: Settings of the slack of the piston cable and recovery for the trials

The piston cable slack is the sum of the free fall height and the recoil compensation of the main cable. Observed penetration is the maximum observed height of sediment on outside core. Computed penetration results from the double integration of the accelerometer versus time. Trials 2, 3, 4 and 5 were performed with various recoil compensation and a constant 2.5m free fall height when trials 1, 3, 6 were performed with various free falls and a constant recoil compensation of 2m

| Trial No. | Free fall | Recoil Compensation | Slack of the Piston Cable | Core No. | Observed Penetration | Computed Penetration | Recovery          | Mean ( $\pm\sigma$ )      | Visual Estimated Quality |
|-----------|-----------|---------------------|---------------------------|----------|----------------------|----------------------|-------------------|---------------------------|--------------------------|
| 1         | 1.5m      | 2m                  | 3.5m                      | K7-01    | > 10m                | —                    | 8.87m             | 8.68 m<br>( $\pm 0.19$ m) | Poor                     |
|           |           |                     |                           | K7-02    | > 10m                | —                    | 8.68m             |                           | Good                     |
|           |           |                     |                           | K7-03    | —                    | 8.1m                 | 8.50m             |                           | Good                     |
| 2         | 2.5m      | 0m                  | 2.5m                      | K7-15    | 10m                  | 6.8m                 | 7.80m             |                           | Poor                     |
| 3         | 2.5m      | 2m                  | 4.5m                      | K7-04    | 7.5m                 | —                    | 6.27m             | 7.72 m<br>( $\pm 1.12$ m) | Good                     |
|           |           |                     |                           | K7-05    | 9m                   | 6.9m                 | 8.38m             |                           | Good                     |
|           |           |                     |                           | K7-06    | 9m                   | 8.1m                 | 8.80m             |                           | Good                     |
|           |           |                     |                           | K7-11    | 10m                  | 9.4m                 | 7.44m             |                           | Poor                     |
| 4         | 2.5m      | 4m                  | 6.5m                      | K7-12    | —                    | not triggered        | not triggered     |                           | —                        |
|           |           |                     |                           | K7-13    | —                    | bent at launching    | bent at launching |                           | —                        |
|           |           |                     |                           | K7-14    | 10m                  | 9.2m                 | 8.70m             |                           | Good                     |
| 5         | 2.5m      | 6m                  | 8.5m                      | K7-09    | 10m                  | 9.1m                 | 5.29m             | 5.23 m<br>( $\pm 0.09$ m) | Poor                     |
|           |           |                     |                           | K7-10    | > 10m                | 8.2m                 | 5.16m             |                           | Very good                |
| 6         | 5m        | 2m                  | 7m                        | K7-07    | 9m                   | 8.3m                 | 7.38m             | 7.11 m<br>( $\pm 0.38$ m) | Very good                |
|           |           |                     |                           | K7-08    | 10m                  | 8.9m                 | 6.84m             |                           | Good                     |

Figure 2: CPT results and estimated lithology



mation of the computed penetration. The observations are not accurate because the traces of silty and sandy sediment on the outside core are not obvious, and also the silty and

sandy lithology and overall the poor sampling frequency of the sensors under-samples the peaks of acceleration, which leads to an underestimation of the displacement.

The recovery ranges from 5 to 9m, namely 54–93% of the maximum recovery. The low standard deviations per trial (except for no. 3) shows the repeatability of the corings. The large discrepancy between the more or less constant penetration and the large range of the averaged per trial recoveries can only be explained by the only variable parameter: the slack of the piston cable (see Section 4).

### 3.3 Core descriptions

The sedimentological description is based on an already studied core<sup>14</sup>. Several marked levels appear from top to bottom: marine gastropods levels (P1 and P2), characteristic successions of hemipelagic, silty and sandy laminae (F1, F2 and F3 in Figure 3). These laminae are distinguishable on the CPT classification. The quality of the 12 cores seems, visually, quite similar to the quality of cores sampled with a steel cable.

### 3.4 Accelerometers records

The behaviour of the foot of the main aramid cable during the elastic recoil is deduced from one specific test (Figure 4). For a water depth of 2000m and a weight of 1t, the elastic recoil is estimated between 3 and 4m for duration

of 1.5 seconds. The initial impulse is disturbed by the tension of the counterweight cable. The platform of release follows the movements of the foot of the cable.

Figure 3: Logs of cores and estimated lithology from CPT

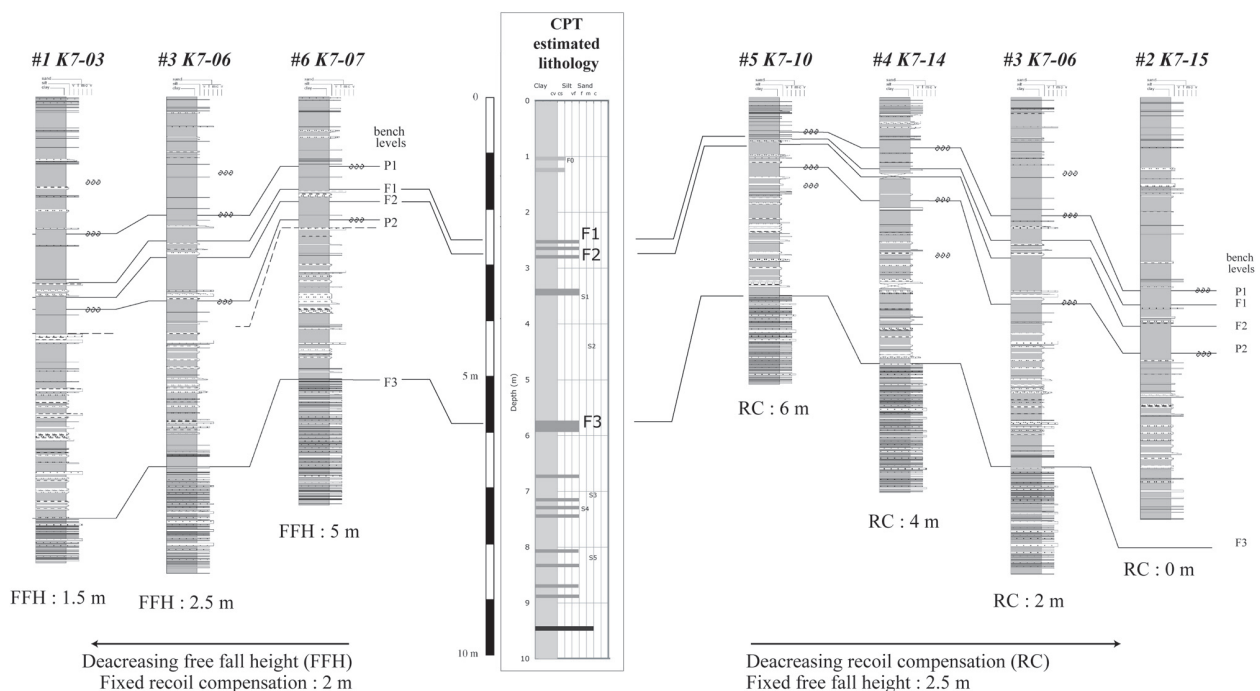


Figure 4: Elastic recoil of the aramid cable

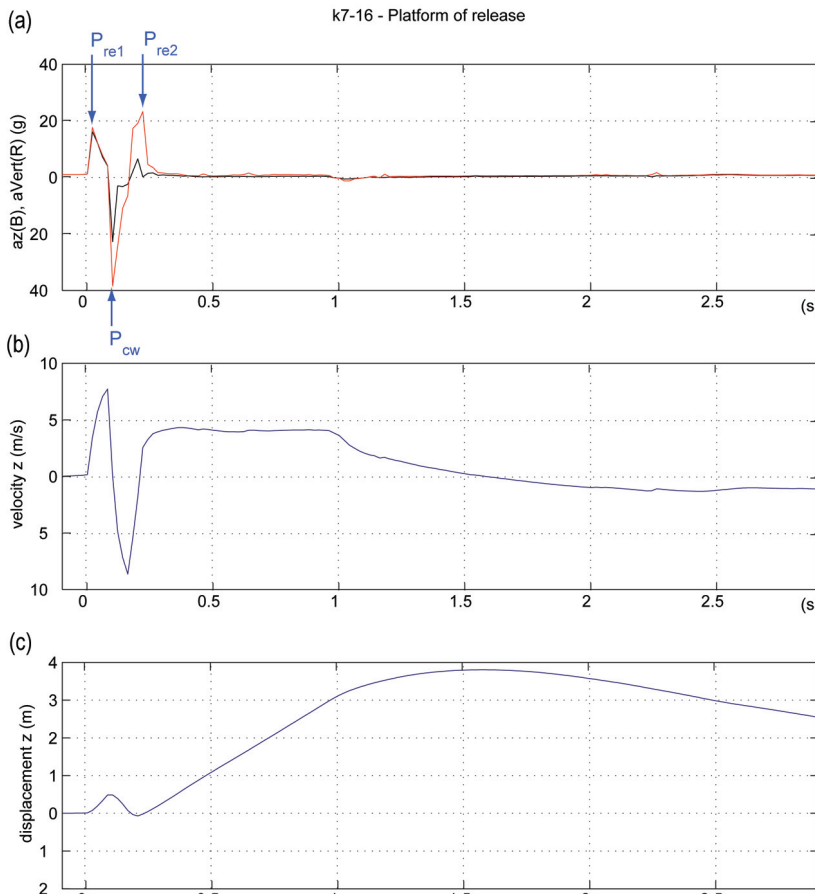
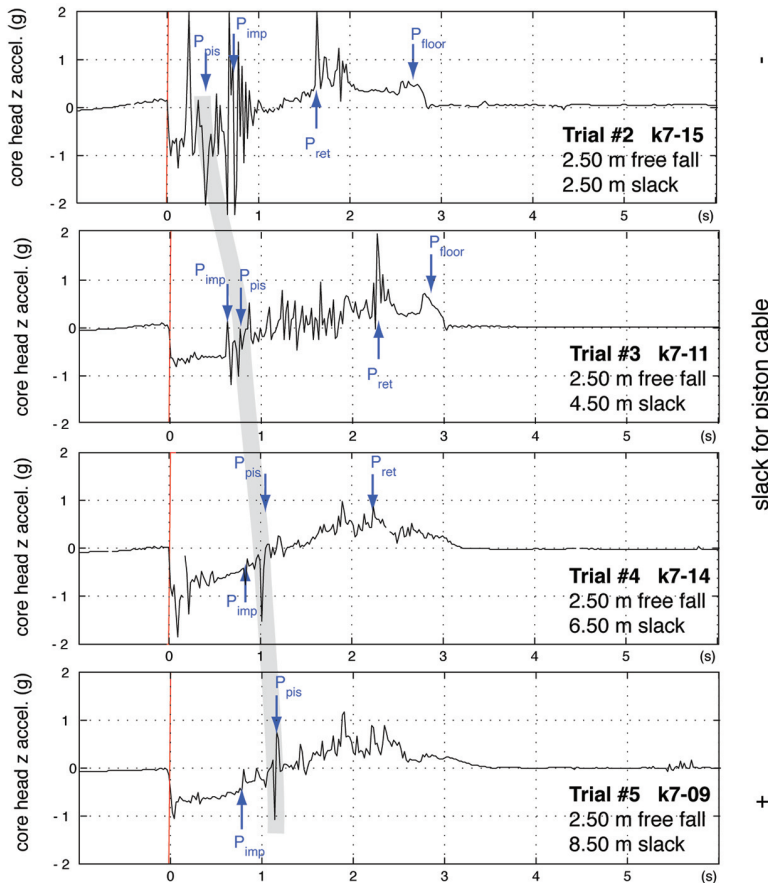


Figure 4 Cont.: (a) Vertical (red) and z-axis (black) acceleration of the platform at the foot of the aramid cable – the vertical acceleration is compounded from the X, Y and Z components; (b) z velocity of the platform computed from a time integration of the vertical acceleration; (c) z displacement of the platform computed from a time integration of the vertical velocity.  $P_{re1}$  and  $P_{re2}$ : peaks due to the elastic recoil of the aramid cable;  $P_{cw}$ : peak due to the tension of the counter-weight cable. The elastic recoil of the main cable lasts 1.4s with 4m of amplitude

The accelerometer on the corer shows that after the triggering, the corer undergoes a continuous slowdown until its full stop (Figure 5). Several characteristic peaks are visible on the records: impact of the core catcher on the seafloor, tension of the piston cable, percussion of the piston at the top of the tube, impact of the weight on the seafloor and impacts into sampled layers. The various piston cable slacks, or the various freefall heights, show fixed and variable peaks through time. This helps to determine the origin of the various peaks (Figure 5).

Figure 5: Behaviour of the corer with four different slacks of piston cable



## 4. Interpretation

### 4.1 Comparison between logs and CPT

The correlation (Figure 3) presents the 3 trials of the decreasing free fall heights series, the 4 trials of the decreasing recoil compensation series and the CPT reference. The bench levels appear at various depths in the cores according to the trials (Figure 3): F1 level varies between 0.70 and 3.80 m; F3 level appears at 3.16 m for the more condensed core (trial 5) when it is not sampled for the more elongated core (trial 2). The ratio of recovered F1-F3 thickness to F1-F3 CPT thickness varies from 0.8 (trial 5) to 1.3 (trial 1) with values close to 1 for trials 6 and 4. The better quality of recovery based on visual check is provided by trials with large slacks (4, 5, 6), when the poorer quality comes from small slacks (1, 2).

Figure 5 Cont.: The peaks appear at the same moment for the four trials except the  $P_{pis}$  which is delayed as the slack increases –  $P_{imp}$ : peak due to the impact of the corer on the seafloor;  $P_{pis}$ : peak due to the tension of the piston cable;  $P_{ret}$ : peak due to the re-tension of the aramid cable;  $P_{floor}$ : peak due to the impact of the weight on the seafloor

Figure 6: Piston status during the coring and quality of the recovered sediment

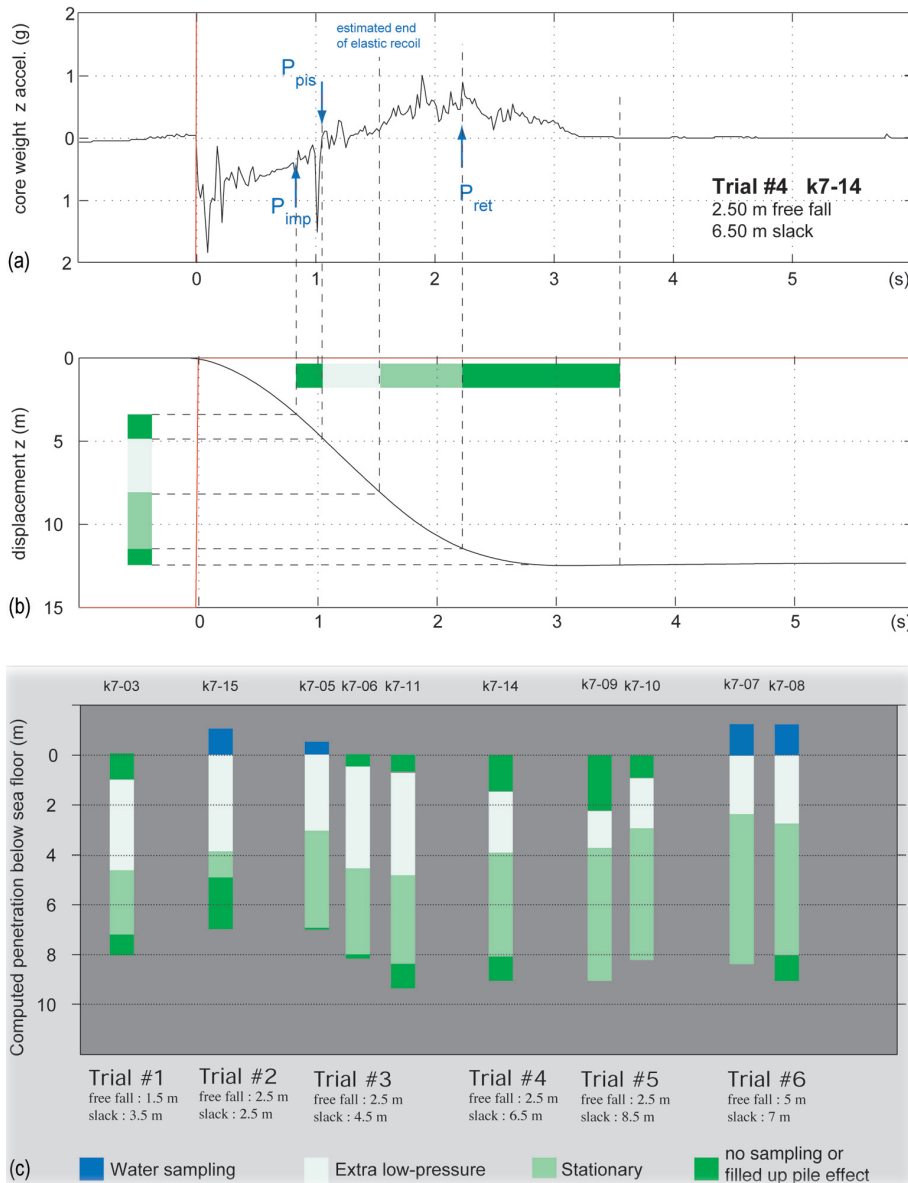
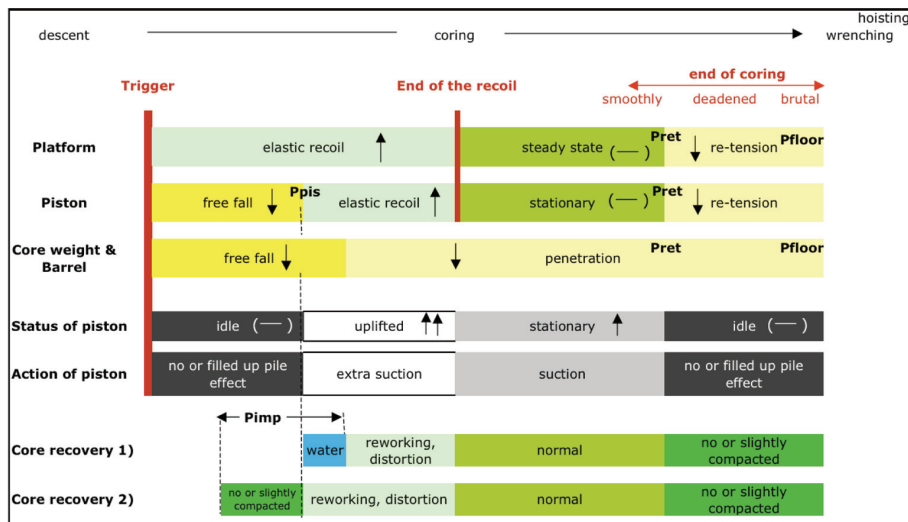


Figure 6 Cont.: (a) example for the accelerometer record for trial 4 (8.7 m of recovery) with the timing of the impact,  $P_{imp}$ , the tension of the piston cable,  $P_{pis}$ , and the re-tension of the aramid cable,  $P_{ret}$ . The duration of the elastic recoil of the aramid cable is 1.4s after the trigger. (b) Piston status of trial 4 derived from the accelerometer curve and from Table 2 versus time (horizontal coloured bar). The piston status versus the penetration (vertical coloured bar) is graphically deduced thanks to the displacement curve coloured code in (c). Uplifted piston and stationary piston occur during 0.4 and 0.8s for 2.5 and 4.4m of penetration, respectively. The remaining part of sediment (1.8m) comes from material sucked during the extra low-pressure phase and the two filled up pile effect phases; and (c) Synthesis of quality of sediment derived from the status of the piston for all the cores

Table 2 Cont.: The horizontal axis represents the few seconds of coring from the triggering to the stop of the core. The three first lines describe the behaviour of the platform of release, the piston and the barrel, and their up, still or down displacements ( $\uparrow$ ,  $\text{—}$ ,  $\downarrow$ ). The status and action of the piston show its relative displacement with regard to the barrel and the consequent action of the piston (no action, suction, extra suction). The latter corresponds to opposite displacements of both the barrel and the piston, while the suction phase corresponds to a stationary piston and a downwards barrel. The action of the piston controls the sediment recovery (no, normal, disturbed and extra sediment). The relative chronology between the impact on the seafloor and the tension of the piston explains the two types of recovery. An extra suction phase before the impact leads to water sampling. The slack of the piston cable allows coordinating the two moments.

Table 2: Behaviour of corer and quality of recovery derived from piston status



#### 4.2 Influence of the cable setting

The correlation of bench levels shows the obvious influence of the setting of the cables of the corer (Figure 3). The shorter the free fall is, the deeper the bench levels are in the core; the smaller the recoil compensation, the deeper the bench levels are in the core. The true geometry of the layers can be obtained by the settings between those of trials 3 and 6 (2m recoil compensation and 4m free fall) or trials 3 and 4 (2.5m free fall and 3m recoil compensation). The results of the two series lead to a setting with recoil compensation smaller than the measured elastic recoil.

#### 4.3 Behaviour of the piston

During the coring operation, the status of the piston determines the suction of the sediment (Table 2, Figure 6). The tension of the piston cable leads the work of the piston. A relaxed cable means an ineffective piston; a tightened cable means the piston creates a depression. After the triggering, the piston is solitary of the corer during the free fall until the piston cable is tightened. Then the piston follows the movements of the platform of release, which goes up via the recoil of the main cable. At that moment, the extra low depression below the piston is due to the combined effects of both the descent of the corer and the ascent of the piston. This period of extra suction corresponds to an over-distortion or at least some distortion phase of sampling. At the end of the recoil, the platform is stabilised because of the behaviour of the aramid cable, and the piston is stationary.

The end of the coring could be smooth, deadened or brutal generating a normal or a slightly compacted sampling due to filled up pile effect. At the very beginning of the coring, the relative chronology between the impact and the tension of the piston cable leads to two different phases: water could be sampled if the impact arrives after the tension of the piston cable. On the contrary, no sampling occurs between the impact time and the piston cable tension. The synthesis for all the cores (Figure 6) show that cores with larger recoil compensations (trials 4 and 5) present longer period with a stationary piston and a consequent better quality, while cores with smaller recoil compensations (trials 1 and 2) present longer period of extra sucked sediment, worse quality and larger recovery.

### 5. Conclusion

The piston facilitates the sampling of sediment during a gravity coring, but also generates disturbances. The understanding of the work of the piston due to accelerometers on corer allows for the highlighting of the key role of the cables setting. Thus, we distinguish four steps during the few seconds of coring, including an optional phase (either water or no sediment sampling), a distortion phase due to an extra suction, followed by a normal sampling phase linked to a stationary piston, and finally an optional compaction phase.

The settings for cores with geotechnical purpose (better quality with a stationary piston) will be different from settings for cores with sedimentological or paleoclimatological purposes (better geometry with a longer ascending piston

phase). A good compromise is to choose a compensation for the slack of the piston cable smaller than the estimated elastic recoil of the main cable.

The understanding of the behaviour of a corer will allow further developments: finding the best settings to have the longer phase with an effective stationary piston; reducing the disturbance and improving the quality or geometry of the recovered sediments; and correcting the depth of layers in the core thanks to modelling the kinematics of the coring.

### References

1. Lancelot Y and Balut Y. (1993). Le carottier 'géant' des TAAF, outil majeur pour la paléocéanographie. In SGF (ed.), Bilan scientifique et prospective pour la fin du siècle. *Géosciences Marines* 16 and 17, décembre, 73.
2. Blomqvist S. (1991). Quantitative sampling of soft-bottom sediments: problems and solutions. *Mar. Ecol. Prog. Ser.* 72(3): 295–304.
3. Thouveny N, Moreno E, Delanghe D, Candon L, Lancelot Y and Shackleton N-J. (2000). Rock magnetic detection of distal ice-rafted debris; clue for the identification of Heinrich layers on the Portuguese margin. *Earth and Planetary Science Letters* 180(1–2): 61–75.
4. Széreméta N, Bassinot F, Balut Y, Labeyrie L and Pagel M. (2004). Oversampling of sedimentary series collected by giant piston corer: evidence and corrections based on 3.5-kHz chirp profiles. *Paleoceanography* 19(PA1005).
5. Skinner LC and McCave IN. (2003). Analysis and modelling of gravity- and piston coring based on soil mechanics. *Marine Geology* 199: 181–204.
6. Lunne T and Long M. (2006). Review of long seabed samplers and criteria for new sampler design. *Marine Geology*, 226: 145–165.
7. Fay JB, Montargès R, Le Tirant P and Brucy F. (1985). Use of the PAM self-boring pressuremeter and the STACOR large sized fixed piston corer for deep seabed surveying In Society for Underwater Technology (SUT). *Proc. Int. Conf. Offshore Site Investigation*. London: SUT, 187–199.
8. Montargès R, Le Tirant P, Wannesson J, Valery P and Berthon JL. (1983). Large size stationary piston corer, Proc. 2nd Deep Offshore Tech. Conf., 63–74.
9. Borel D, Puech A, Dendani H and de Ruijter M. (2002). High quality sampling for deep water geotechnical engineering: the STACOR experience, Ultra Deep Engng and Tech., Brest, France, 18–20 June.
10. Lunne T, Berre T and Strandvik S. (1998). Sample disturbance effects in deep water soil investigations. In Society for Underwater Technology (SUT). *Offshore Site Investigation and Foundation Behaviour – 'New Frontiers'*. London: SUT, 199–220.
11. Meunier J, Sultan N, Jegou P and Harmegnies F. (2004). First Tests of Penfeld: a New Seabed Penetrometer. In Chung J, Izumiyama K, Sayed M and Hong S (eds). *Proc. of the 14th Int. Offshore and Polar Engng Conf.*, Toulon, France, 23–28 May 2004. Danvers, MA: ISOPE, 338–345.
12. Douglas BJ and Olsen RS. (1981). Soil classification using electric cone penetrometer. Cone Penetration Testing and Experience, Proc. ASCE National Convention, St Louis, 209–27.
13. Robertson PK. (1990). Soil classification using the cone penetration test. *Canadian Geotech. J.* 27: 151–158.
14. Migeon S, Savoye B and Faugeres J-C. (2000). Quaternary development of migrating sediment waves in the Var deep-sea fan: distribution, growth pattern, and implication for levee evolution. *Sedimentary Geology* 133: 265–293.